Fundamental frequency PWM control of IGBT clamped three phase nine levels inverter topology for photovoltaic system

Rabiaa Mechouma
LEB Laboratory, University of Batna 2, Algeria
Rabiaa.mechouma@yahoo.com

Boubekeur Azoui
LEB Laboratory, University of Batna 2, Algeria
azoui_b@yahoo.com

Sabir Ouchen
LGEB, University of Biskra, Algeria
Sabir_ouchen@yahoo.fr

***Abstract*—The multilevel multi-string inverter has gained much attention in recent years due to its advantages in lower switching loss, better electromagnetic compatibility, higher voltage capability, and lower harmonic distortion. Solar Energy is one of the favorable renewable energy resources and the multilevel inverter has been proven to be one of the important enabling technologies in photovoltaic (PV) utilization. As the number of levels increases, it is important to control more switches in parallel with their concurrent processing capability. This paper proposes an IGBT clamped three phase nine levels photovoltaic inverter topology with a multicarrier dual reference pulse-width modulated (PWM) control scheme. Four carrier waves of the fundamental frequency and different amplitudes are compared with two references (a sine wave and its opposite) for generating the control signals of the switches. Some DC/DC boost converters are used to amplify the voltage produced by the photovoltaic generators. Each of these converters is controlled by an MPPT algorithm in order to track the maximum power point of the GPV. Results of simulation in Matlab environment are given and discussed.**

***Index Terms*— Photovoltaic (PV) system, multilevel three phase multi-string inverter, IGBT clamped inverter, multicarrier PWM.**

I. INTRODUCTION

The ever growing demand for renewable energy resources is gaining importance day by day. Wind, Solar, etc. are some examples of such renewable energies. It is expected that by 2050, 60% of our energy requirement will be supplied by these renewable energy resources [1]. Due to this reason, now our focus is on inventing new topologies of improved inverters. Among these topologies multilevel inverter with multiple PWM control is gaining more importance. It has gained much attention in recent years due to its advantages in lower switching loss, better electromagnetic compatibility, higher voltage capability and lower harmonic distortion. Multilevel inverters include an array of power semiconductors and capacitor voltage sources, the output of which generates voltages with stepped waveforms. Photovoltaic (PV), wind energy and hydro conversion are the most explored technologies due to their considerable advantages [2-4], such as reliability, reasonable installation and energy production costs, low environmental impact, capability to support micro grid systems and to connect to the electric grid [5]. In this paper, we present an IGBT clamped three phase nine level inverter designed for photovoltaic system. This inverter is controlled by a PWM strategy based on the comparison of several carrier waves with two reference signals. More control signals are obtained. Instead of a single photovoltaic generator at the input of the inverter, we have a multiple continuous source which is composed of several photovoltaic generators. Each of them consists of N_P branches, each of which is composed of N_S solar panels in series. Each generator of this source generates a voltage which is amplified at the output by means of a dc / dc converter. This converter is controlled by an MPPT algorithm. The overall system is shown in Fig. 1. The study is simulated in Matlab / Simulink and followed by a simulation and discussion of results.

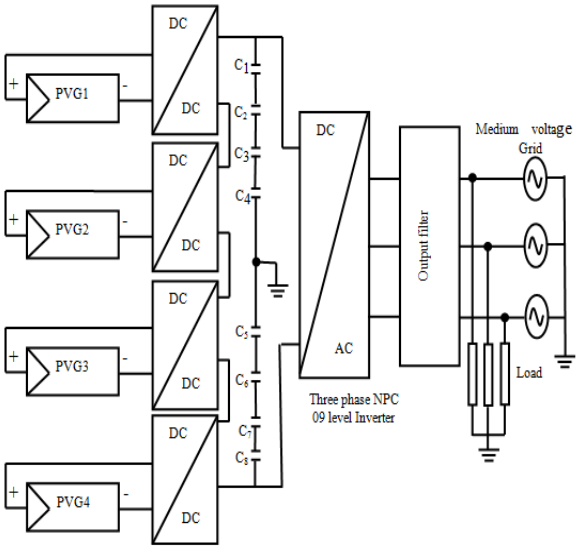

Fig. 1. Schematic diagram of the overall PV system

I. MODELLING OF THE GLOBAL GRID CONNECTED PHOTOVOLTAIC SYSTEM STRUCTURE

Modeling photovoltaic system is required as a crucial step to describe the functioning of all the elements that are all starting from the DC source arriving to the grid. It predicts the conceptual and energy performance of PV systems connected to the grid in different climatic conditions and

under well-defined loads. Models of the various components will be presented as follows:

A. Model of the photovoltaic source

As already mentioned, the photovoltaic source consists of 04 parts, each of which represents a partial photovoltaic generator. Each partial PVG generates at its output a DC voltage which is then amplified by a DC / DC converter. Continuous output voltages of the converters are then summed to obtain an overall voltage that feeds the inverter. The equivalent circuit diagram of a PV cell is illustrated in Fig. 2.

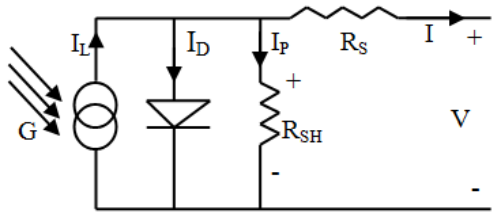

Fig. 2. Equivalent circuit diagram of a PV cell

The selected model in this work is inspired from references [6-8]. The advantage of this model is that it can be established using only standard data for the module and cells provided by the manufacturer in the technical data sheet (data and graphs). It is independent of the saturation current I_S of the diode (see Fig. 2). The current supplied by the solar module (I_M) in any conditions, is given by:

$$I_M = I_{SCM}\left[1-\left\{\exp\left(\frac{V_M - V_{OCM} + I_M R_{SM}}{nV_{THM}}\right) - \exp\left(\frac{-V_{OCM}}{nV_{THM}}\right)\right\}\right]. \quad (1)$$

Where:

I_{SCM} and V_{OCM} are respectively the short circuit current and the open circuit voltage at the STC (Standard Test Conditions), I_M and V_M are current and voltage respectively delivered by the module at any conditions, R_{SM} is the series resistance of the module, V_{THM} is the thermal voltage and n is the quality factor which varies typically from 1 to 2.

V_{OCM} and I_{SCM} are given by:

$$V_{OCM} = V_{OCC} \times N_{SC} \quad (2)$$

$$I_{SCM} = I_{SCC} \times N_{PC} \quad (3)$$

The thermal voltage is given by:

$$V_{THM} = V_{THC} \times N_{SC} \quad (4)$$

Where: $V_{THC} = \frac{kT_C}{q}$

The series resistance of the module is given by:

$$R_{SM} = \frac{N_{SC}}{N_{PC}} R_{SC} \quad (5)$$

Where:

V_{THC} is the thermal voltage of the PV cell, R_{SC} is the series resistance of the PV cell, k is the Boltzmann's constant (equal to 1.3806×10^{-23} J/K), q is the electrical charge of the electron with a value 1.602×10^{-19} C, N_{PC} is the number of branches of cells in parallel in a module and N_{SC} is the cells number of each branch.

The open circuit voltage of the PV cell is given by:

$$V_{OCC} = V_{OCC-ref} - \beta(T - T_{ref}) \quad (6)$$

Where: $V_{OCC-ref}$ is the open circuit voltage of the PV cell in standard conditions, T_{ref} is the reference value of the temperature (T_{ref}=25°C) and T is the operating temperature of the PV cell, it is given by:

$$T = T_a - T_{ref} \quad (7)$$

T_a is the ambient temperature of the PV cell.

The thermal voltage of the PV cell can be easily calculated using the coordinates of the maximum power point of the cell (V_{MPPC} and I_{MPPC}). The expression of V_{THC} can have the following formula:

$$V_{THC} = \frac{V_{MPPC} + R_{SC} I_{MPPC} - V_{OCC}}{\mathrm{Ln}\left(1 - \frac{I_{MPPC}}{I_{SCC}}\right)} \quad (8)$$

The current delivered by each PVG (which is composed of N_P branches of modules in parallel with N_s modules) is given by the following expression:

$$I = N_P I_{SCM}\left[1-\left\{\exp\left(\frac{N_S V_M - N_S V_{OCM} + N_P I_M R_{SM}}{nN_S V_{THM}}\right) - \exp\left(\frac{-V_{OCM}}{nV_{THM}}\right)\right\}\right] \quad (9)$$

B. DC/DC Boost converter and its control

1) DC/DC Boost converter model

A boost converter (step-up converter) is a DC-to-DC power converter with an output voltage greater than its input voltage. A schematic of a boost power stage is shown in Fig. 3. The basic principle of a Boost converter consists of two distinct states.

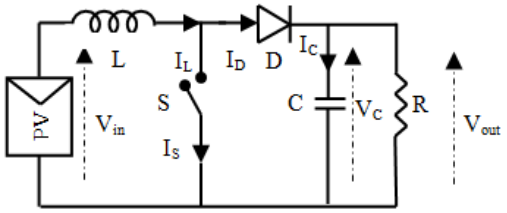

Fig. 3. Boost converter schematic

In continuous mode, the current through the inductor (I_L) never falls to zero. The output voltage can be calculated as follows, in the case of an ideal converter (i.e. using components with an ideal behavior) operating in steady conditions [9].

During the On-state, the switch "S" is closed, which makes the input voltage (V_{in}) appears across the inductor, which causes a change in current (I_L) flowing through the inductor during a time period (t) as it is shown by this formula:

$$\frac{\Delta I_L}{\Delta t} = \frac{V_{in}}{L} \quad (10)$$

At the end of the On-state, the increase of I_L is therefore:

$$\Delta I_{L_{ON}} = \frac{1}{L}\int_0^{DT} V_{in}dt = \frac{DT}{L}V_{in} \qquad (11)$$

Where: D is the duty cycle; it represents the fraction of the commutation period T during which the switch is On. Therefore D ranges between 0 (S is never on) and 1 (S is always on).

During the Off-state, the switch "S" is open, so the inductor current flows through the load. If we consider a zero voltage drop in the diode, and a capacitor large enough for its voltage to remain constant, the evolution of I_L is:

$$V_{in} - V_{out} = L\frac{dI_L}{dt} \qquad (12)$$

Therefore, the variation of I_L during the Off-period is:

$$\Delta I_{L_{OFF}} = \int_{DT}^{T} \frac{(V_{in} - V_{out})dt}{L} = \frac{(V_{in} - V_{out})(1-D)T}{L} \qquad (13)$$

As we consider that the converter operates in steady-state conditions, the amount of energy stored in each of its components has to be the same at the beginning and at the end of a commutation cycle. In particular, the energy stored in the inductor is given by:

$$E = \frac{1}{2}LI_L^2 \qquad (14)$$

So, the inductor current has to be the same at the start and the end of the commutation cycle. This means the overall change in the current (the sum of the changes) is zero:

$$\Delta I_{L_{ON}} + \Delta I_{L_{OFF}} = 0 \qquad (15)$$

Substituting $\Delta I_{L_{ON}}$ and $\Delta I_{L_{OFF}}$ by their expressions yields:

$$\Delta I_{L_{ON}} + \Delta I_{L_{OFF}} = \frac{V_{in}DT}{L} + \frac{(V_{in} - V_{out})'1-D)T}{L} = 0 \qquad (16)$$

This can be written as:

$$\frac{V_{out}}{V_{in}} = \frac{1}{1-D} \qquad (17)$$

This, in turn, reveals the duty cycle to be:

$$D = 1 - \frac{V_{in}}{V_{out}} \qquad (18)$$

(Where: $0 \le D \le 1$), we have:

$$V_{out} = \frac{1}{C}\int I_{out}dt \qquad (19)$$

This after derivation becomes:

$$\frac{dV_{out}}{dt} = \frac{1}{C}(I_L - \frac{V_{out}}{R}) = \frac{1}{C}[I_L - \frac{1}{R}(\frac{V_{in}}{1-D})] \qquad (20)$$

Where: L, R and C are respectively the inductor, the resistor and the capacitor of the DC / DC converter, V_{in} and V_{out} are respectively the input voltage and the output voltage of the DC/DC converter. The efficiency $\eta_{DC/DC}$ of the boost DC/DC converter is given by:

$$\eta_{dc/dc} = \frac{V_{out} \times I_{out}}{V_{in} \times I_{in}} = \frac{P_{out}}{P_{in}} \qquad (21)$$

2) MPPT Control

The boost (step-up) DC / DC converter is modeled as a block whose inputs are the voltage delivered by the solar modules and the second input is the current generated by the Maximum Power Point Tracking (MPPT) controller. This MPPT is used on the basis of a search algorithm called perturb and observe (P & O) [10].

C. Model of the IGBT clamped three-Phase nine levels Inverter

Fig. 4 shows the diagram of the IGBT clamped *three-Phase nine levels* inverter. This inverter is composed of three arms each of which itself composed of ten IGBT that are noted as "S_{ij}". The index (i) indicates the phase: if (i = 1), it means the phase "A", if (i=2), it means the phase "B" and if (i=3), it means the phase "C". Upper part of the arm in each phase and the switches noted as: S'_{i1}, S'_{i2}, S'_{i3}, S'_{i4} and S'_{i5} form the lower part of the arm.

The inverter also includes other switches noted as "Q_{ij}" switches that are clamped to the voltage divider and the neutral point. The inverter can generate 09 voltage levels: four levels are positive, one level is zero and four levels are negative. It is composed of 54 switches, hence the necessity of 54 control signals. These signals can be generated by a PWM controller.

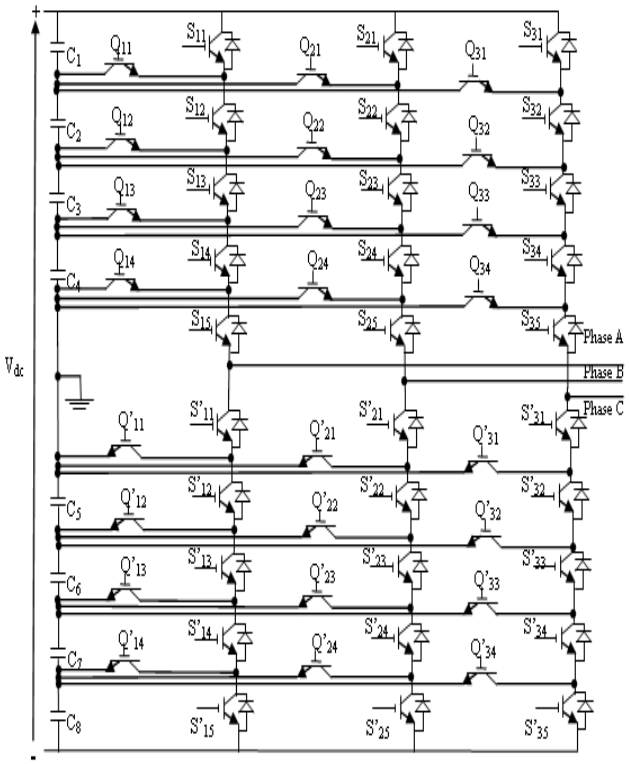

Fig. 4. Diagram of the IGBT clamped three-Phase nine levels Inverter

D. Control circuit of the inverter

The control circuit of the inverter is shown in Fig.5. It is based on the use of the PWM strategy in a closed loop current. This strategy consists of comparing four carrier signals of the same frequency with two reference sinusoidal waves (the sinusoidal wave and its opposite). In addition a closed loop control is performed for each phase using a PID controller which is characterized by its coefficients K_i and K_p (K_i=0.06; K_p=0.01). A square signal is added.

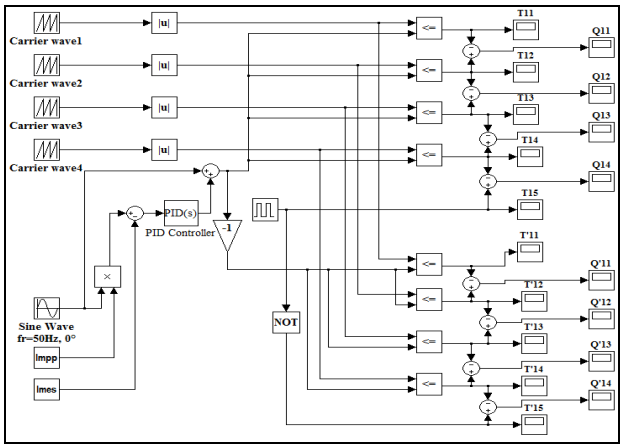

Fig. 5. Control circuit of one arm of the inverter (Phase "a")

II. SIMULATION OF THE OVERALL SYSTEM

The overall diagram of the simulation is shown in Fig. 6

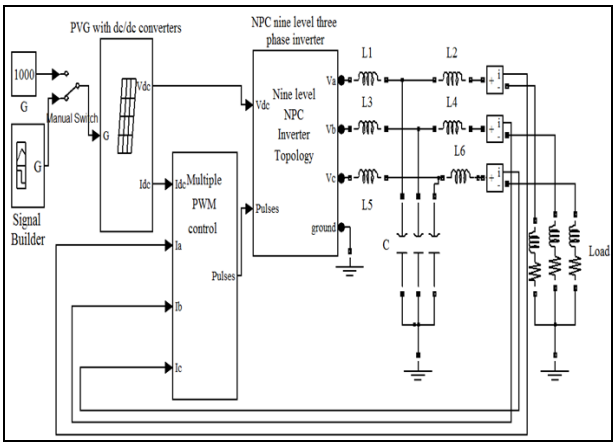

Fig. 6. Simulation scheme of the overall PV system

The simulation scheme consists of the main component inverter powered by the photovoltaic source under solar radiation which intensity is chosen constant (1000W/m^2) or variable with the use of the tool called (Signal Builder). An "LC" filter is placed at the output of the inverter for supplying an "RL" load. The switch control signals are obtained by the multiple PWM technique (see Fig .5).

The simulation diagram of the partial photovoltaic generator with DC/DC boost converter is illustrated in Fig.7.

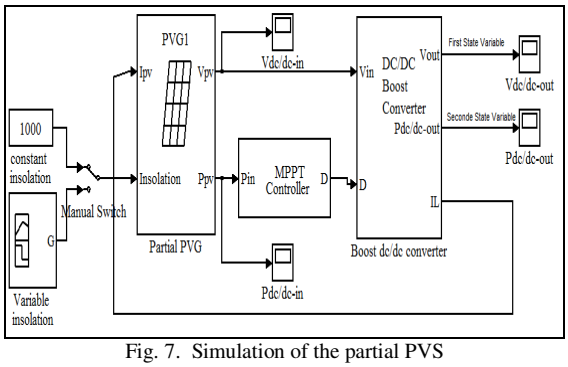

Fig. 7. Simulation of the partial PVS

A. Parameters of the partial photovoltaic generator

The characteristics of the partial PVG are given in Fig.8:

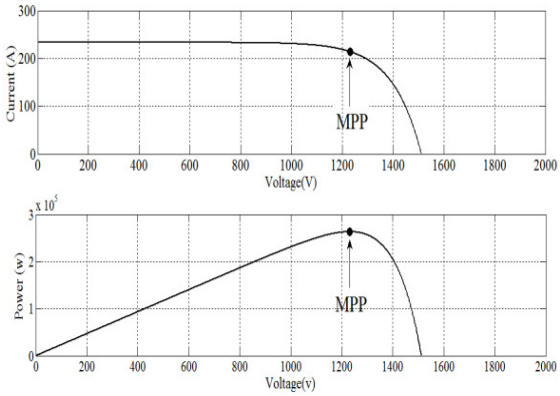

Fig. 8. Characteristics of the partial PVG

B. Parameters of the DC/DC boost converter

The parameters of the dc / dc converter are illustrated in Fig.9 and Fig.10. In Fig.9 a significant amplification of the voltage was observed, it passes from 1211V to the input of the dc/dc converter to a value of 3120V at its output.

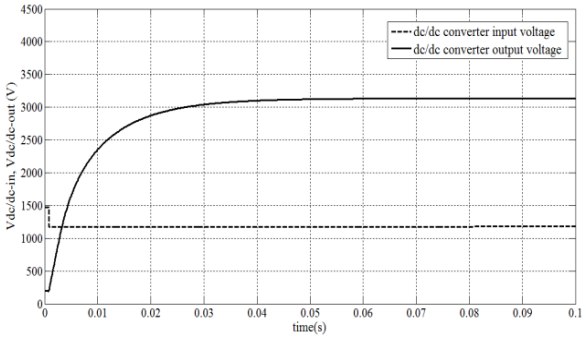

Fig. 9. DC/DC boost converter input and output voltage in partial PV system

We recall that we have 04 partial generators (see Fig.1), and then the total voltage at the input of the inverter is given by 3120 × 4=12480V.

Fig.10 shows the dc/dc converter input and output power.

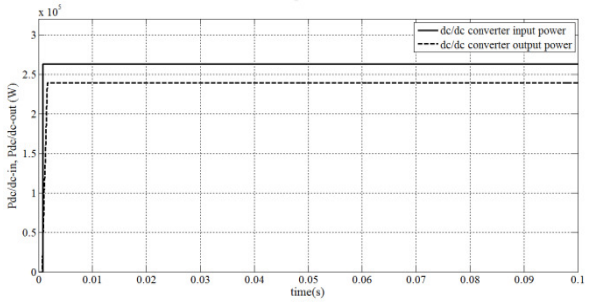

Fig.10. DC/DC boost converter input and output power in partial PV system

The power delivered by the photovoltaic generator to the input of dc/dc converter is equal to 262.5kW, giving a total power produced by the four generators of 262.5×4=1.05MW. The power output of each dc/dc Converter is 239,1kW, then the power supplied to the inverter input is 239.1×4=956.4kW. The efficiency of each dc/dc Converter is given by:

$$\eta_{dc/dc} = (239.1/262.5)=0.91$$

C. Parameters of the Inverter

The parameters of inverter are voltage and current at its output. These parameters are shown in the Fig.12 and Fig.13 as follows:

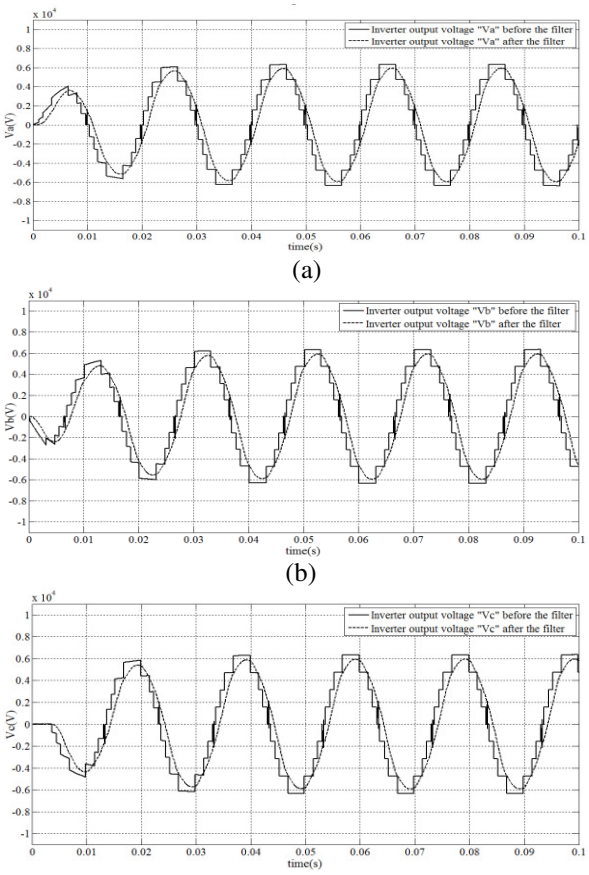

Fig.11. Inverter output voltage before and after the filter: (a) Va, (b) Vb, (c) Vc

Fig.11 shows the voltages Va, Vb and Vc at the output of the inverter before and after the filter. It is clear that the tension before the filter is shaped staircase and that after the filter has a sinusoidal shape but with a very short delay time (0.001sec).

Fig.12 and Fig.13 show the inverter output currents Ia, Ib and Ic before and after the filter.

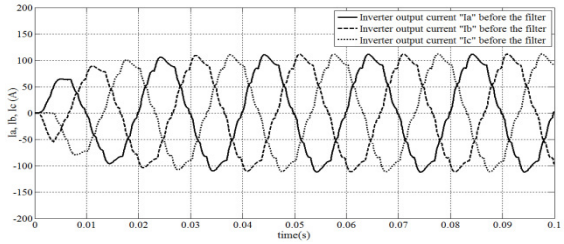

Fig. 12. Inverter output currents: Ia, Ib, Ic before the filter

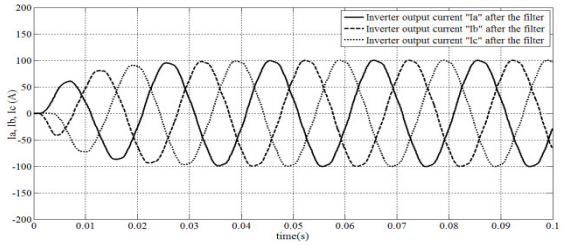

Fig. 13. Inverter output currents: Ia, Ib, Ic after the filter

Currents of the three phases after the filter are almost sinusoidal with an amplitude value of 100A, but they suffer from a delay 0.001sec compared to current before filtering.

Fig.14 shows the inverter efficiency which is equal to:

$\eta_{inv} = 0.96$.

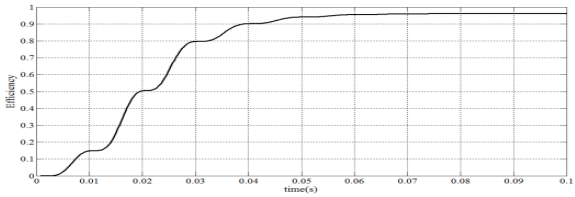

Fig.14. Inverter efficiency

D. Fast Fourier Transform (FFT) analysis

The Fast Fourier Transform (FFT) analysis, using the POWERGUI block, yields to the following results:

Table 1
THE THD (%) OF THE VOLTAGE AND THE CURRENT OF PHASE "a" FOR FUNDAMENTAL FREQUENCY "FC=50HZ"

Phase "a"	**THD(%)**
Ianf	5.86
Iaf	2.48
Vanf	12.90
Vaf	2.48

In table 1, the Total Harmonic Distortion (THD) is given for phase "a" for fundamental frequency (50Hz).

Where: fc is the carrier wave frequency in PWM control. Ianf and Vanf are respectively the unfiltered inverter current and voltage of the phase "a", Iaf and Vaf are respectively the filtered inverter current and voltage of the phase "a". The THD value is given by Fig.15.

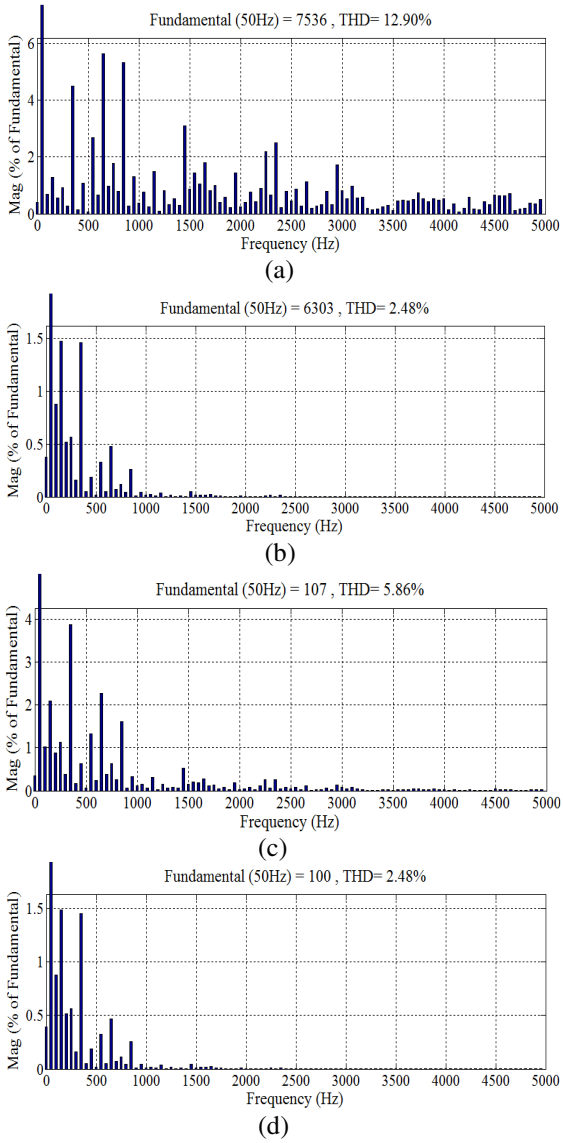

Fig.15. Spectrum of the inverter output voltage and current after the filter for phase "a"

(a) Spectrum of output voltage Vanf
(b) Spectrum of output current Ianf
(c) Spectrum of output voltage Vaf
(d) Spectrum of output voltage Iaf

As we see the THD has a value of 2.48% for voltage and current. This is a very acceptable value, although the PWM control has been achieved with a fundamental frequency, we can say that this is a very satisfactory result.

III. CONCLUSION

In this paper, an IGBT-clamped nine level three phase photovoltaic inverter topology has been proposed and studied. It is a new topology where clamped diodes and flying capacitors were replaced by IGBTs. The number of switches in an inverter arm was largely reduced as follow:

- In the diode-clamped nine level topology, the number of switches was sixteen (16) while in an inverter arm it becomes ten (10) in the IGBT -clamped topology.
- The number of pairs of diodes clamped which was ten pairs (20 diodes), this has been reduced to four pairs in IGBTs clamped (08 IBGTs).

The importance of this study is that the PWM strategy was based on a comparison of only four carrier signals with two reference signals (a sinusoidal signal and its opposite) instead of eight triangular carrier signals in the case of the clamped diodes inverter. Also, in this control, switching frequency has been sufficiently reduced; it is taken as the fundamental frequency (50 Hz). So, the control of all switches was so easy.

The proposed topology is economical compared with diode-clamped and flying capacitors topologies.

We can conclude that the obtained results seem quite interesting and acceptable. The inverter efficiency was 96% and THD was less than 3%.

REFERENCES

[1] Lai J.S. and Peng F.Z, "Multilevel Inverters: A survey of topologies, Controls, and Applications", IEEE Trans.Ind.Elec. Vol. 49, pp. 724-738, Aug. 2002.

[2] F. Kininger, "Photovoltaic systems technology". Kassel, Germany: Universität Kassel, Institut für Rationelle Energiewandlung, 2003. Available at: www.uni-kassel.de/re.

[3] I.S. Jacobs and C.P. Bean, world energy statistics - 2009", International Energy.

[4] R.Mechouma, H.Aboub and B. Azoui, "Multicarrier wave dual reference very low frequency PWM control of a nine levels NPC multi-string three phase inverter topology for photovoltaic system connected to a medium electric grid", Upec 2014, 2 - 5 September 2014, Cluj-Napoca, Romania.

[5] "Global Market Outlook for Photovoltaics Until 2014", European Photovoltaic Industry Association (EPIA). Available at: www. epia.org.

[6] A.D. Hansen et al., "Models for Standalone PV Systems", Report Riso-R-1219(EN) SEC, RNL, Roskilde, Denmark, 2000.

[7] L. Castaner et S. Silvester, "Modeling Photovoltaic Systems Using PSPICE", Wily, 1ère Édition ISBN 0-470-84528-7, 2002.

[8] A.N.Celik et N.Acikgoz, "Modeling and Experimental Verification of the Operating Currents of Mono-Cristalline Photovoltaic Modules Using Four and Five Parameters Models", Applied Energy, Vol.84, pp. 1-15, Issue 1, January 2007.

[9] Carl. Nelson & Jim. Williams, "Boost Converter Operation", LT1070 Manuel Design, Application Note 19, Jun. 1986.

[10] J. Surya Kumari, Dr. Ch. Sai Babu, A. Kamalakar Babu, "Design and Analysis of P&O and IP&O MPPT techniques for Photovoltaic System", International Journal of Modern Engineering Research (IJMER), Vol.2, Issue.4, pp.2174-2180. Jul. /Aug. 2012.